Dense One-shot 3D Reconstruction by Detecting Continuous Regions with Parallel Line Projection

Ryusuke Sagawa
AIST
Tsukuba, Japan
ryusuke.sagawa@aist.go.jp

Hiroshi Kawasaki, Shota Kiyota
Kagoshima University
Kagoshima, Japan
kawasaki@ibe.kagoshima-u.ac.jp

Ryo Furukawa
Hiroshima City University
Hiroshima, Japan
ryo-f@hiroshima-cu.ac.jp

Abstract

3D scanning of moving objects has many applications, for example, marker-less motion capture, analysis on fluid dynamics, object explosion and so on. One of the approach to acquire accurate shape is a projector-camera system, especially the methods that reconstructs a shape by using a single image with static pattern is suitable for capturing fast moving object. In this paper, we propose a method that uses a grid pattern consisting of sets of parallel lines. The pattern is spatially encoded by a periodic color pattern. While informations are sparse in the camera image, the proposed method extracts the dense (pixel-wise) phase informations from the sparse pattern. As the result, continuous regions in the camera images can be extracted by analyzing the phase. Since there remain one DOF for each region, we propose the linear solution to eliminate the DOF by using geometric informations of the devices, i.e. epipolar constraint. In addition, solution space is finite because projected pattern consists of parallel lines with same intervals, the linear equation can be efficiently solved by integer least square method. In this paper, the formulations for both single and multiple projectors are presented. We evaluated the accuracy of correspondences and showed the comparison with respect to the number of projectors by simulation. Finally, the dense 3D reconstruction of moving objects are presented in the experiments.

1. Introduction

Active 3D scanning methods using just a single image with static light pattern (*a.k.a.* one-shot scan) have attracted many people, because of its exclusive advantages, i.e., it can capture extremely fast motion, such as dynamic fluid motion or object's explosion by simply increasing the frame-rate and the shutter-speed of the camera. Based on such background, it has been intensively researched and several products are commercialized recently. For example, Kinect [14] is one of the recent successful product with well-balanced accuracy, resolution and cost effectiveness. Although Kinect can be efficiently used for the purpose of motion capture and gesture recognition, 3D quality is not enough for modeling and inspection. Similarly, other one-shot scanning techniques are also usually insufficient for modeling purpose either with resolution, accuracy or stability.

Recently, grid-based one-shot scanning techniques are proposed and achieved both high accuracy and stability by unique encoding technique, i.e. positional information are encoded into the connectivity of grid lines. However, it has a severe problem for practical usage that is sparse reconstruction. The main reason of the sparse reconstruction is that the 3D reconstruction is only realized with detected curves of grid lines. In addition, if the total amount of connections between detected curves is not enough, shapes cannot be reconstructed correctly and reconstruction becomes sparser.

In this paper, we propose the technique to solve the abovementioned problems to achieve high-density and high-speed reconstructions of dynamic objects. For solution, two approaches are presented as follows:

1. Efficient image processing technique to detect continuous regions from a single image.
2. Region based 3D reconstruction method using geometric constraint to achieve stable and dense reconstruction.

Thanks to the proposed techniques, all the pixels of continuous region are used for reconstruction to increase density and stability, whereas only intersection points are used in the previous grid-based reconstruction. Further, since many areas which are not connected to other areas by detected curves are connected together as the single region with our technique, reconstruction areas increase significantly and calculation becomes stable. In the experiments, we actually construct the system, which consists of a single or multiple projectors and one camera, and successfully reconstructed

the series of entire shape of dynamically moving object and fluid surfaces. We also conducted both qualitative and quantitative evaluations. The contribution of our technique is as follows.

1. Phase estimation to segment continuous region are efficiently realized by Gabor filter.
2. Efficient formulation and solution to eliminate DOF of phase ambiguity using geometric constraint(epipolar constraint) are proposed.
3. Efficient calculation techniques using integer least square method to improve solution and stability are presented.
4. It is shown and proved by experiments that the technique is new solution for dense and fast motion reconstruction.

2. Related work

Shape reconstruction techniques using projector and camera system have been widely researched and developed [2]. Main issue for projector and camera based 3D scanning system is how to get correspondences between them. For solution mainly two methods are known, such as temporal encoding method and spatial encoding method.

Since techniques using temporal encoding method is easy to implement, accurate, dense and robust, it has commonly been used thus far [4, 10, 3]. However, there is one severe drawback exist for the technique, that is, it requires multiple images with different patterns projected onto the object, and thus, it is not suitable for high-speed capturing. Recently, several methods for high-speed capturing were proposed by using a DLP projector and a high-speed camera [21, 15] or reducing the required number of patterns using both temporal and spatial changes [9, 22]. However, these approaches works for objects that have either limited speeds or rigid body assumption.

Some methods use projectors only to provide textures that change over time and 3D information is restored using a passive stereo technique [6, 24], although they are not strictly structured light systems. Since they still require several patterns for identification, they are not suited for extremely fast objects.

Techniques using only spatial encoding of a pattern are suitable for fast-moving objects, since they use only a single-frame image [11, 20]. On the other hand, the problems are that they typically need complex patterns or colors to encode positional information. To determine the spatial codes uniquely, the size of a code becomes large. Such patterns are easily affected by textures, shape discontinuities, image compression caused by tilted surfaces. Therefore, density of patterns should be inevitable low, and thus, 3D reconstructions tend to be sparse and unstable.

Recently, the solution for the complex pattern by using a simple grid pattern which embeds information in relation of connection of parallel lines has been published [12, 16, 19]. However, projected lines should be detected as separated curves on the captured image, and thus, interval of grid pattern tends to be large and density is inevitably low, e.g. several times of pixel width. Our technique provides a simple solution by interpolating lines with Gabor filter.

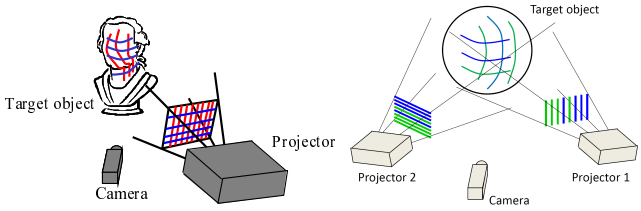

(a) (b)

Figure 1. (a) A system with one camera and one projector, (b) A system with one camera and two projectors.

In the paper, we also propose the technique to eliminate the remaining ambiguity of estimated phase; one may notice that the process is as same as the phase unwrapping process in phase-shifting methods [8, 21]. In reality, the technique is also a solution for phase unwrapping process using geometric information (epipolar constraint in this case) instead of using several different phases in previous ones. One important difference from previous phase unwrapping technique and ours is that we only require two phase images, and thus, by assigning two colors for each phase image, we can realize phase unwrapping process with a single image.

3. Overview

The system of the proposed method consists of one camera and single/multiple projectors as shown in Fig. 1. Since the camera and projectors are assumed to be calibrated, the intrinsic and extrinsic parameters of the devices are known. Because the proposed method uses a fixed pattern emitted from the projectors, no synchronization is required between the camera and the projectors.

In the case of a system that uses a single projector (Fig. 1(a)), the projector casts two sets of parallel lines that are along the vertical and horizontal axis of the projector image, respectively. In the case that a system has two projectors (Fig. 1(b)), each projector cast a set of parallel lines. For both cases, the projected lines form a grid pattern on the surface of a target object. The proposed method reconstructs the shape from the grid pattern captured by the camera.

Although the 3D reconstruction from a grid pattern proposed in [7] basically works without any information added to the line pattern, a spatial encoding is useful to improve the robustness of 3D reconstruction. A periodic color code based on the de Bruijn sequence [11, 17, 23] was introduced to the grid-based reconstruction in [16]. In this paper, instead of using the color-code ID assigned to each line in

the pattern directly, we propose a method to find the dense phase assigned to each pixel of the camera image. Based on this phase information, we formulate the problem of 3D reconstruction as estimating a variable assigned to each region of the phase by solving a linear equation.

4. Detecting continuous regions by color-coded line patterns

In this section, we explain the proposed method to detect continuous regions in a camera image by decoding color-coded line patterns projected onto an object. The procedure consists of the following steps:

1. Find the curves in a camera image, which are the projection of parallel lines in a projector image.
2. Decode the periodic pattern that is encoded by using colors.
3. Compute the phase of periodic pattern for each pixel by interpolating the code.
4. Detect regions in which the phase is continuous.
5. Unwrap the phase in each region.

Fig. 2 shows an example of the result at each step of the image processing. (a) is the input image with projecting two line sets. (b) is the result of curve detection for the one of the line sets. The ID of each curve in a periodic color pattern is represented by the line color in (c). By interpolating the IDs, the phase at each pixel is computed as shown in (d). The continuous regions detected by using the phase are represented by the color in (e). The phase in each region is unwrapped as shown in (f).

4.1. Finding curves for parallel lines emitted from a projector

The pattern emitted from one or multiple projectors consists of multiple sets of parallel lines. First, we detect a set of curves in a camera image as the projection of parallel lines by discriminating them from the other sets of curves. We use the direction and color of curves for discrimination.

The curve detection is based on the method proposed in [16]. It classifies pixels to three labels based on the derivative along an axis of the image: positive, negative, and nearly zero. The position of a curve is the peak of intensity and detected as the boundary of the labels between positive and negative. While the position is computed in subpixel accuracy in [16] by using the cost of belief propagation, the subpixel position is computed by the interpolation of curves described in the following sections in this paper. Therefore, we simplify the method to use two labels, positive (P) and negative (N), and determine the labels by the energy minimization of the following cost function by graph cuts.

Now, we assume to detect nearly vertical curves in a camera image without loss of generality. We rotate the image to detect curves of other directions. Additionally, the color of lines are encoded by using two of RGB colors, for example blue and cyan, in this paper. In this case, all lines have blue component and curves are detected by using blue plane of the camera image. The cost function is defined as

$$\sum_{p \in V} g(l_p) + \lambda \sum_{(l_p, l_{p'}) \in E} h(l_p, l_{p'}), \tag{1}$$

where V is the set of pixels and E is the set of 4-neighbor pixel pairs. l_p is the label assigned to the pixel p. λ is a parameter defined by user. The data cost $g(p)$ is defined as follows:

$$g(l_p) = \begin{cases} -D(p) & \text{if } l_p \text{ is P} \\ D(p) & \text{if } l_p \text{ is N} \end{cases} \tag{2}$$

where $D(p)$ is the derivative of the intensity along the horizontal axis. The discontinuity cost $h(l_p, l_{p'})$ depends on the direction of $\overrightarrow{pp'}$. In the case that it is along the vertical axis, $h(l_p, l_{p'}) = 0$ if the labels are the same, and $h(l_p, l_{p'}) = 1$ otherwise. In the case that it is along the horizontal axis,

$$h(l_p, l_{p'}) = \tag{3}$$
$$\begin{cases} -\text{sgn}(D(p)) + \text{sgn}(D(p')) & \text{if } l_p \text{ is P and } l_{p'} \text{ is N} \\ \text{sgn}(D(p)) - \text{sgn}(D(p')) & \text{if } l_p \text{ is N and } l_{p'} \text{ is P} \\ 0 & \text{otherwise.} \end{cases}$$

Finally, the curves in an input image are detected at the boundary between the labels P and N.

4.2. Decoding periodic color pattern

The lines are encoded by a periodic code based on the de Bruijn sequence, which is defined by the number of colors q and the length of the code n. Namely, once the colors of the adjacent n curves are determined, the curves are identified in the periodic code of length q^n. In this paper, $q = 2$ and $n = 3$.

Decoding of the periodic code, based on a method proposed in [16], is done with a graph created by vertical and horizontal curves and their intersection points. The labels of curves are determined by energy minimization by using belief propagation. On the other hand, we create a graph by vertical curves and lines along the horizontal axis of the image. Thus, the color codes of different sets of curves are decoded separately without computing intersection points. Even if the number of curve sets is more than two, the decoding can be done without change.

4.3. Compute the phase of periodic pattern

Since the number of lines in a cycle is $q^n = 8$ since $q = 2$ and $n = 3$, the IDs of curves are assigned from 0 to 7. They are integer values and assigned for the pixels on the curves. The values for the pixels that are not on the curves can be computed by interpolating the curves, and it is considered as the phase of the periodic function.

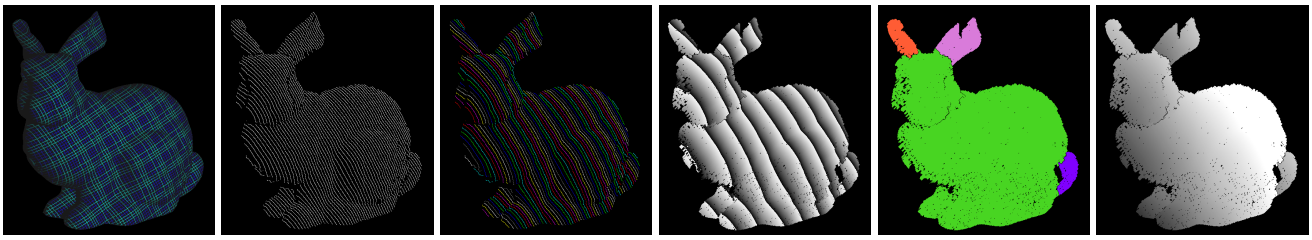

(a) (b) (c) (d) (e) (f)

Figure 2. An example of the result at each step of the image processing: (a) an input image, (b) the detected curves for a set of parallel lines, (c) the decoding result of the periodic pattern, (d) the computed phase by interpolating the code, (e) the detected continuous regions, and (f) the unwrapped phase in each region.

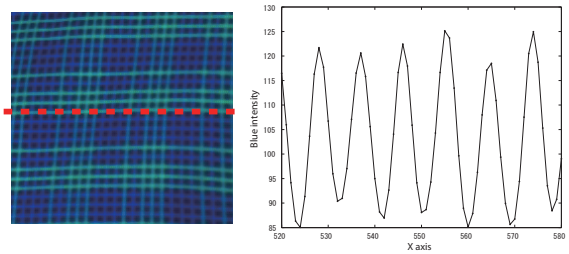

Figure 3. The intensity profile of blue component is assumed as a sine function along the dotted red line.

Fig. 3 shows an example of the intensity profile of blue component along the dotted red line. The peaks of curves are sparse in the image and the intensity profile is nearly periodic function. We assume a locally planar surface for the surface model, and thus, we can use a complex Gabor filter to interpolate phase between the curves with sub-pixel accuracy. Since Gabor filter is used for detecting a specific band of frequency in a local region, the wavelength is required. In the paper, the interval of curves L is used for wavelength. The results is a complex value z and the phase ψ is calculated by $\psi = \arctan(\Im z / \Re z)$. If the IDs of two curves are k and $(k+1) \mod q^n$, the phase of periodic code ϕ at the pixel becomes $\phi = k + \psi/2\pi$. Since this is also done for the pixels on the line, the position of a curve is calculated in subpixel accuracy.

4.4. Detecting continuous regions and unwrapping the phase

After the computation of the phase of each pixel, the proposed method segments the image into regions that have continuous phase. It determines if two 4-connected pixels are in the same region by solving

$$\min(|d|, |d + q^n|, |d - q^n|) < \tau, \tag{4}$$

where $d = \phi_1 - \phi_2$, ϕ_1 and ϕ_2 are the phases of the considered pixels and τ is a user defined threshold. The algorithm for segmentation is based on the two-pass algorithm of connected component labeling. In the first pass, the neighboring pixels are labeled as the same region if they satisfies Eq. (4), and the equivalence between neighboring labels are stored. The neighboring labels are relabeled based on the equivalence information in the second pass. If the area of a region is smaller than a threshold, the method removes it as a noisy region after segmentation.

After finding continuous regions, the phase is unwrapped in each region. Consequently, each pixel in the region has the corresponding coordinate of the projector with a common unknown shift. Once the unknown shift is estimated by the method described in the next section, the correspondence between a camera pixel and a projector line is determined. Then, the 3D points are calculated by triangulation. In the latter part of this paper, we call the unwrapped phase a relative projector coordinate.

Finally, the relative projector coordinate is multiplied by the interval between lines in the projector image. Then, the scale of coordinate is adjusted to the coordinate of projector image.

5. Formulating grid-based 3D reconstruction with continuous regions

The next step of grid-based 3D reconstruction is estimating the correspondence between curves in the camera image and lines in the projector image. The previous method, presented in [7], estimates parameter of each curve, the number of parameters is equal to the number of curves. While in this paper, continuous regions based on grid line pattern are detected by the method described above. The number of unknown parameters is only one for each region. In this section, we explain the formulation of estimating parameters with continuous regions.

5.1. Formulation for 3D reconstruction with one projector

First, we explain the case with one projector. In this case, two sets of lines are parallel to vertical and horizontal axes of the projector image, respectively. If the regions of both patterns are detected at a pixel of the camera image, the pixel (x_c, y_c) has the correspondence with a relative projector coordinate (u, v), where u and v are the coordinates calculated from vertical and horizontal curves. Fig. 4

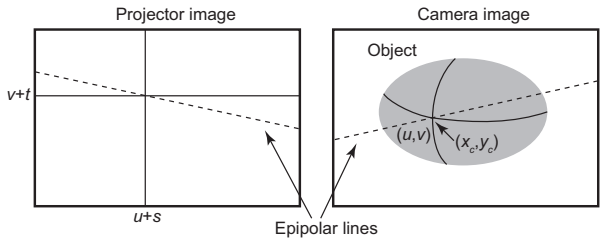

Figure 4. The pixel (x_c, y_c) has the correspondence with a relative projector coordinate (u, v). The pixel corresponds to a pixel $(u + s, v + t)$ in the projector image based on the epipolar geometry with the unknown shift (s, t).

shows this situation. This correspondence gives the following epipolar constraint:

$$[u+s, v+t, 1]F \begin{bmatrix} x_c \\ y_c \\ 1 \end{bmatrix} = 0, \tag{5}$$

where F is the fundamental matrix between the camera and projector, and s and t are unknown shift for the regions of vertical and horizontal curves, respectively. Since the unknown variables in this equation are only s and t, Eq. (5) is a linear equation. This equation is obtained for all pixels that have u and v. The parameters are shared by the pixels in the same region. If the number of regions of vertical and horizontal curves are N_s and N_t, the following simultaneous linear equation is obtained:

$$A\boldsymbol{x} = \boldsymbol{b}, \quad \boldsymbol{x} = [s_1, \ldots, s_{N_s}, t_1, \ldots, t_{N_t}]^T, \tag{6}$$

where A is the coefficient matrix and b is the vector of constant terms. The number of variables are $N_s + N_t$, which is much smaller than the number of curves in the camera image.

If A is full rank, a unique solution is obtained. Since each row of A means the epipolar line at $(u + s, v + t)$, A is full rank if they are not parallel. In the previous formulation in [7], the solution by linear equation has 1-DOF ambiguity. Therefore, they solve the ambiguity by matching projected pattern and detected curves, in which the knowledge of line interval was used. Since the lines used in the proposed method have constant interval and the knowledge is used in detecting continuous regions, the unique solution is given only by linear equation in our formulation.

5.2. Formulation for 3D reconstruction with multiple projectors

Second setup of grid-based 3D reconstruction is projecting parallel line sets from different projectors [13]. We formulate a setup with two projectors based on epipolar geometry. If the points of projector 1 and 2 corresponding to a camera point (x_c, y_c) are $(u + s, s')$ and $(v + t, t')$, respectively, the epipolar constraints are expressed as follows:

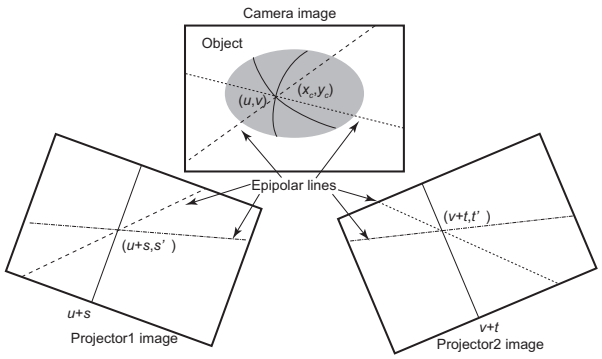

Figure 5. The relationship between three corresponding points are given by the epipolar geometry. s' and t' are expressed by linear polynomials of s and t.

$$[u+s, s', 1]F_1[x_c, y_c, 1]^T = 0 \tag{7}$$

$$[v+t, t', 1]F_2[x_c, y_c, 1]^T = 0 \tag{8}$$

$$[u+s, s', 1]F_{12}[v+t, t', 1]^T = 0 \tag{9}$$

In this formulation, each projector emits a set of lines parallel to the vertical axis of the projector image. If the direction of lines is different, the representation of projector points can be modified without loss of generality. This situation is illustrated in Fig. 5. The corresponding points are defined by the three pairs of epipolar lines. By using u and v given by the region detection, s' and t' are expressed by linear polynomials of s and t from Eq. (7) and (8), respectively. Therefore, Eq. (9) consists of the terms of st, s, t and constant.

To make Eq. (9) linear, we introduce a new variable $r = st$ to replace the second-order term. Eq. (9) can be regarded as a linear equation of r, s and t. Similar to Eq. (6), r, s and t can be solved by gathering the constraints of all points.

In the method presented in [13], although it is proposed that the constant interval of lines is used as an additional constraint, this constraint is already incorporated in the region detection. While the previous method have restriction on the configuration of camera and projectors to apply the constraint, the proposed method solves by linear equation regardless of configuration between camera and projectors.

The proposed formulation can be extended to the case of three or more projectors. If m projectors are used, a pair of patterns are chosen out of them and the constraint equations are created by using the regions of the pair. The simultaneous equation is obtained by using ${}_m\mathrm{C}_2$ combinations of patterns.

Since the nonlinear constraint $r = st$ is omitted from the system in the above linear solution, the obtained solution may not satisfy it in some cases. Especially, it happens when the regions of three or more patterns are overlapped. Therefore, we use the linear solution as an initial guess and improve it by nonlinear minimization of Eq. (9).

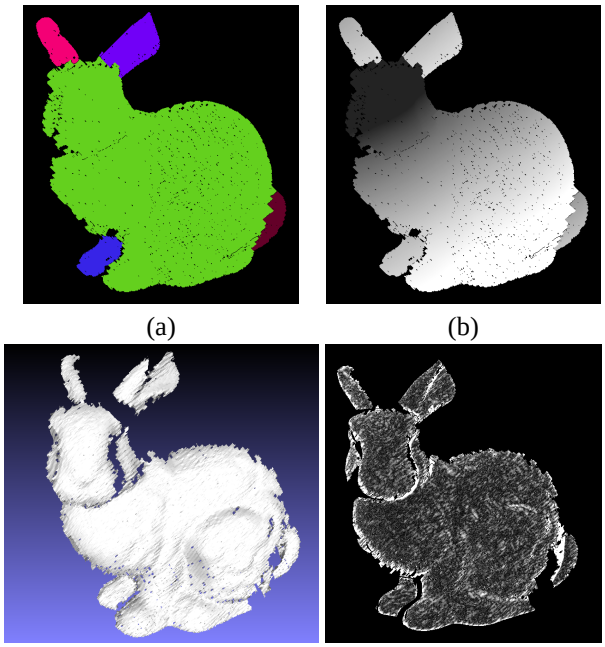

(a) (b) (c) (d)

Figure 6. The results of segmentation and relative projector coordinate for the other line sets are shown in (a) and (b), respectively. (c) is the result of 3D reconstruction. The error of the computed projector coordinate is shown in (d).

5.3. Solution by Integer Least Square

If the projector coordinate $(u+s, v+t)$ is estimated, it should match with the phase of periodic code determined in the region detection. The solution, however, can be different due to the error of calibration and image processing. To constrain the solution so that it matches with the detected phase, we transform the variables as follows:

$$s = Lq^n\tilde{s}, \quad t = Lq^n\tilde{t}, \tag{10}$$

where L is the interval of lines in the projector image, which is 5 or 10 in this paper. Now, the constraint becomes that the new variables $\tilde{s}$ and $\tilde{t}$ should be integer.

The problem becomes an integer least square (ILS) problem, which the linear equation is solved under the constraint that the solution must be integer. It is known that this problem occurs in the case of GPS measurement [18]. In this paper, we implemented an ILS solver based on one of the solver, MILES [5], to obtain $\tilde{s}$ and $\tilde{t}$.

6. Experiments

In the experiments, we first test the proposed method by simulating the system. The camera image is generated by using a virtual object and illumination simulated by a ray tracing tool. We used as model, the bunny, from Stanford University [1].

The input image with one projector is shown in Fig. 2(a).

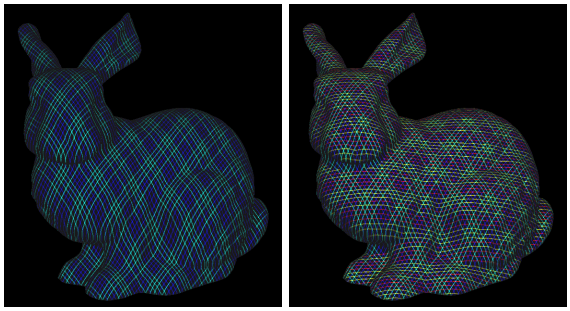

(a) (b)

Figure 7. The object is illuminated by (a) two and (b) three projectors, respectively.

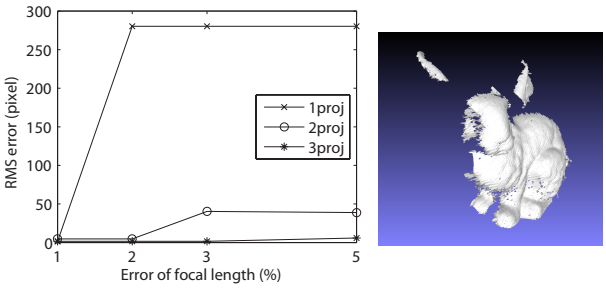

Figure 8. (Left) The errors of corresponding points are compared with respect to the number of projectors by adding the calibration error to the focal length of the camera. (Right) If the error of focal length is 5%, the phase cycles of some parts are wrongly estimated in the case of one/two projectors.

Two sets of parallel lines, which are along the axes, are projected on to the object. The result of region detection for the one of the sets is shown in Fig. 2(e) and (f). The result for the other set is Fig. 6(a) and (b). The numbers of regions for the sets are four and five, respectively. The number of variables in Eq. (6) is nine in this case, which is a quite small number for a problem of finding correspondences to reconstruct a non-parametric 3D shape. The reconstructed shape is shown in Fig. 6(c). To estimate the accuracy of the proposed method, we compare the projector coordinate for each pixel computed by the proposed method with the ground truth. Fig. 6(d) shows the difference between the computed coordinate and the ground truth. The bright pixels indicate large errors. The pixels at the occluding boundary have large errors. While the root-mean-square (RMS) error of the projector coordinate is 1.02 pixels if all pixels are used, it becomes 0.175 pixels if the boundary pixels are omitted from the computation. This result shows that the proposed method can find the correspondence in subpixel accuracy by interpolating the phase if the surface looks toward the camera and projector enough to calculate the color code.

Second, we test the 3D reconstruction with multiple projectors. Fig. 7(a) and (b) show the input images with two and three projectors, respectively. One of the projectors is

the one used in the single projector case. If the color code is detected correctly, the error in finding correspondences is mainly caused by the error of calibration. In this experiment, we compare the robustness of correspondences by modifying the focal length of the camera parameter from the ground truth as the calibration error.

Fig. 8 shows the RMS errors of correspondences by comparing the cases with one, two, and three projectors. The field of view of the camera is about 56 degrees, and we changed the focal length by 1, 2, 3, and 5% of the ground truth. The result shows that the system with three projectors is the most robust since the phases for the most of the regions are correctly estimated. The reason is that redundant informations to solve Eq. (7),(8), and (9) are given in this case. In the case of two projectors, the phase cycles of some parts are different from the ground truth as shown in Fig. 8(right) if the error of focal length is larger than 2%. In the case of one projector, the error to estimate phase cycles occurs if the error of focal length is larger than 1%.

The difference between the cases of one and two projectors is that the axes of pattern planes are places at skew position in the case of two projectors, while they intersect each other in the case of one projector. The axis means a line that is shared by 3D planes formed by parallel line pattern [7]. As discussed in [13], the robustness of linear solution is improved if the axes are at skew position, which is a reason why the case of two projectors gave better results. The further analysis will be in future work.

Third, we experiment the proposed method by using real cameras and projectors. As mentioned in the introduction, one of the advantage of one-shot 3D scanning is suitable to capture the shape of objects in fast motion. In this experiments, we chose as target to capture the shape: water splash, deforming cloth, and deforming face. The image sequences were captured at 60-2000 FPS by using a high speed camera. The objects are illuminated by a single projector. The image sizes of the camera and projector are 1024×1024 and 1024×768 pixels, respectively.

Fig. 9 shows the four frames of the input images and results from the three sequences. In the case of water splash (a), the water was white and opaque and the pattern was reflected on its surface. The proposed method succeeded to capture the shape of water splash and wave caused by the ball. In the case of deforming cloth (b), the detailed shape, such as wave and crease caused by hitting a ball, was captured. In the case of face (c), the cheek was hit by hand, and we can observe the deformation from the captured shape. The advantage of the proposed method is that it is applicable even though the motion of the targets are very fast, and additionally targets are textureless. The average computational time was 5.00, 6.15, and 3.15 seconds for each frame by Intel Xeon 2.4GHz processor.

7. Conclusion

This paper describes a method to reconstruct dense 3D shapes from a single image of projected grid pattern. The proposed method detects continuous regions by calculating dense phase information from a set of parallel lines that are periodically encoded by colors. Since the number of variables to be estimated is only one for each region, the total number of variables becomes very small. Finding correspondence is formulated by a simultaneous linear equation based on epipolar geometry. The solution is obtained by the integer least square of the equation. The formulations are given for the cases of both single and multiple projectors. In the experiments, we evaluated the accuracy of correspondences and the comparison with respect to the number of projectors by simulation. The 3D reconstruction of moving objects are shown in the real experiments. In future work, we plan to improve the computational time toward real-time reconstruction.

Acknowledgment

This work was supported in part by SCOPE No.101710002, Grant-in-Aid for Scientific Research No.21200002 and NEXT program No.LR030 in Japan.

References

[1] The Stanford 3D Scanning Repository. http://www-graphics.stanford.edu/data/3Dscanrep/. 6

[2] J. Batlle, E. Mouaddib, and J. Salvi. Recent progress in coded structured light as a technique to solve the correspondence problem: a survey. Pattern Recognition, 31(7):963–982, 1998. 2

[3] K. L. Boyer and A. C. Kak. Color-encoded structured light for rapid active ranging. IEEE Trans. on PAMI, 9(1):14–28, 1987. 2

[4] D. Caspi, N. Kiryati, and J. Shamir. Range imaging with adaptive color structured light. IEEE Trans. on PAMI, 20(5):470–480, 1998. 2

[5] X.-W. Chang and T. Zhou. MILES: MATLAB package for solving Mixed Integer LEast Squares problems. GPS Solutions, 11(4):289–294, 2007. 6

[6] J. Davis, D. Nehab, R. Ramamoorthi, and S. Rusinkiewicz. Spacetime stereo: A unifying framework for depth from triangulation. IEEE Transactions on Pattern Analysis and Machine Intelligence (PAMI), 27(2):296–302, Feb. 2005. 2

[7] R. Furukawa, H. Kawasaki, R. Sagawa, and Y. Yagi. Shape from grid pattern based on coplanarity constraints for one-shot scanning. IPSJ Transaction on Computer Vision and Applications, 1:139–157, 2009. 2, 4, 5, 7

[8] J. Gühring. Dense 3-d surface acquisition by structured light using off-the-shelf components. In Videometrics and Optical Methods for 3D Shape Measurement, volume 4309, pages 220–231, 2001. 2

[9] O. Hall-Holt and S. Rusinkiewicz. Stripe boundary codes for real-time structured-light range scanning of moving objects. In ICCV, volume 2, pages 359–366, 2001. 2

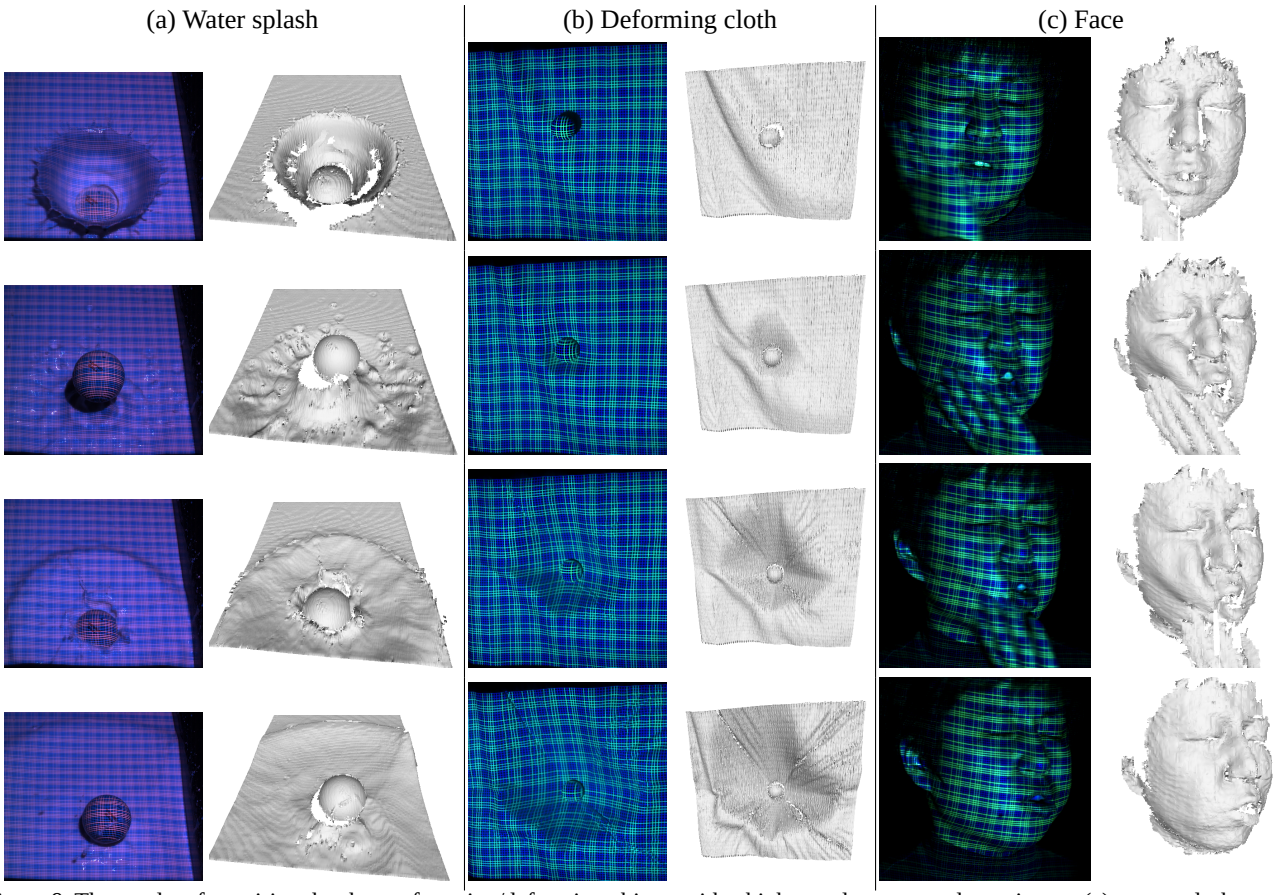

Figure 9. The results of acquiring the shape of moving/deforming objects with a high speed camera and a projector: (a) water splash caused by a ball, (b) deforming cloth hit by a ball, and (c) deforming face hit by hand.

[10] S. Inokuchi, K. Sato, and F. Matsuda. Range imaging system for 3-D object recognition. In ICPR, pages 806–808, 1984. 2

[11] C. Je, S. W. Lee, and R.-H. Park. High-contrast color-stripe pattern for rapid structured-light range imaging. In ECCV, volume 1, pages 95–107, 2004. 2

[12] H. Kawasaki, R. Furukawa, , R. Sagawa, and Y. Yagi. Dynamic scene shape reconstruction using a single structured light pattern. In CVPR, pages 1–8, June 23-28 2008. 2

[13] H. Kawasaki, R. Furukawa, R. Sagawa, Y. Ohta, K. Sakashita, R. Zushi, Y. Yagi, and N. Asada. Linear solution for oneshot active 3d reconstruction using two projectors. In 3DPVT, 2010. 5, 7

[14] Microsoft. Xbox 360 Kinect. http://www.xbox.com/en-US/kinect. 1

[15] S. Narasimhan, S. Koppal, and S. Yamazaki. Temporal dithering of illumination for fast active vision. In European Conference on Computer Vision, volume 4, pages 830–844, October 2008. 2

[16] R. Sagawa, Y. Ota, Y. Yagi, R. Furukawa, N. Asada, and H. Kawasaki. Dense 3d reconstruction method using a single pattern for fast moving object. In ICCV, 2009. 2, 3

[17] J. Salvi, J. Batlle, and E. M. Mouaddib. A robust-coded pattern projection for dynamic 3D scene measurement. Pattern Recognition, 19(11):1055–1065, 1998. 2

[18] P. Teunissen. The least-squares ambiguity decorrelation adjustment: a method for fast GPS ambiguity estimation. Journal of Geodegy, 70:65–82, 1995. 6

[19] A. O. Ulusoy, F. Calakli, and G. Taubin. One-shot scanning using de bruijn spaced grids. In The 7th IEEE Conf. 3DIM, 2009. 2

[20] P. Vuylsteke and A. Oosterlinck. Range image acquisition with a single binary-encoded light pattern. IEEE Trans. on PAMI, 12(2):148–164, 1990. 2

[21] T. Weise, B. Leibe, and L. V. Gool. Fast 3D scanning with automatic motion compensation. In Proc. IEEE Conference on Computer Vision and Pattern Recognition, pages 1–8, 2007. 2

[22] M. Young, E. Beeson, J. Davis, S. Rusinkiewicz, and R. Ramamoorthi. Viewpoint-coded structured light. In CVPR, June 2007. 2

[23] L. Zhang, B. Curless, and S. Seitz. Rapid shape acquisition using color structured light and multi-pass dynamic programming. In Proc. First International Symposium 3D Data Processing Visualization and Transmission, pages 24–36, 2002. 2

[24] L. Zhang, N. Snavely, B. Curless, and S. M. Seitz. Spacetime faces: High-resolution capture for modeling and animation. In ACM Annual Conference on Computer Graphics, pages 548–558, August 2004. 2